



This is a repository copy of  *$\beta$ -glycerophosphate, not low magnitude fluid shear stress, increases osteocytogenesis in the osteoblast-to-osteocyte cell line IDG-SW3.*

White Rose Research Online URL for this paper:

<https://eprints.whiterose.ac.uk/215584/>

Version: Published Version

---

**Article:**

Owen, R. [orcid.org/0000-0003-1961-0733](https://orcid.org/0000-0003-1961-0733), Wittkowske, C. [orcid.org/0009-0004-9702-5913](https://orcid.org/0009-0004-9702-5913), Lacroix, D. [orcid.org/0000-0002-5482-6006](https://orcid.org/0000-0002-5482-6006) et al. (2 more authors) (2024)  $\beta$ -glycerophosphate, not low magnitude fluid shear stress, increases osteocytogenesis in the osteoblast-to-osteocyte cell line IDG-SW3. *Connective Tissue Research*, 65 (4). pp. 313-329. ISSN 0300-8207

<https://doi.org/10.1080/03008207.2024.2375065>

---

**Reuse**

This article is distributed under the terms of the Creative Commons Attribution (CC BY) licence. This licence allows you to distribute, remix, tweak, and build upon the work, even commercially, as long as you credit the authors for the original work. More information and the full terms of the licence here:

<https://creativecommons.org/licenses/>

**Takedown**

If you consider content in White Rose Research Online to be in breach of UK law, please notify us by emailing [eprints@whiterose.ac.uk](mailto:eprints@whiterose.ac.uk) including the URL of the record and the reason for the withdrawal request.



[eprints@whiterose.ac.uk](mailto:eprints@whiterose.ac.uk)  
<https://eprints.whiterose.ac.uk/>



## $\beta$ -glycerophosphate, not low magnitude fluid shear stress, increases osteocytogenesis in the osteoblast-to-osteocyte cell line IDG-SW3

Robert Owen, Claudia Wittkowske, Damien Lacroix, Cecile M. Perrault & Gwendolen C. Reilly

To cite this article: Robert Owen, Claudia Wittkowske, Damien Lacroix, Cecile M. Perrault & Gwendolen C. Reilly (10 Jul 2024):  $\beta$ -glycerophosphate, not low magnitude fluid shear stress, increases osteocytogenesis in the osteoblast-to-osteocyte cell line IDG-SW3, Connective Tissue Research, DOI: [10.1080/03008207.2024.2375065](https://doi.org/10.1080/03008207.2024.2375065)

To link to this article: <https://doi.org/10.1080/03008207.2024.2375065>



© 2024 The Author(s). Published by Informa UK Limited, trading as Taylor & Francis Group.



Published online: 10 Jul 2024.



Submit your article to this journal [↗](#)



Article views: 235



View related articles [↗](#)



View Crossmark data [↗](#)

# $\beta$ -glycerophosphate, not low magnitude fluid shear stress, increases osteocytogenesis in the osteoblast-to-osteocyte cell line IDG-SW3

Robert Owen <sup>a,b,c</sup>, Claudia Wittkowske <sup>b,d</sup>, Damien Lacroix <sup>b,d</sup>, Cecile M. Perrault <sup>b,d</sup>, and Gwendolen C. Reilly <sup>a,b</sup>

<sup>a</sup>Department of Materials Science and Engineering, University of Sheffield, Sheffield, UK; <sup>b</sup>INSIGNEO Institute for In Silico Medicine, University of Sheffield, Sheffield, UK; <sup>c</sup>School of Pharmacy, University of Nottingham Biodiscovery Institute, University of Nottingham, Nottingham, UK; <sup>d</sup>Department of Mechanical Engineering, University of Sheffield, Sheffield, UK

## ABSTRACT

**Aim:** As osteoblasts deposit a mineralized collagen network, a subpopulation of these cells differentiates into osteocytes. Biochemical and mechanical stimuli, particularly fluid shear stress (FSS), are thought to regulate this, but their relative influence remains unclear. Here, we assess both biochemical and mechanical stimuli on long-term bone formation and osteocytogenesis using the osteoblast-osteocyte cell line IDG-SW3.

**Methods:** Due to the relative novelty and uncommon culture conditions of IDG-SW3 versus other osteoblast-lineage cell lines, effects of temperature and media formulation on matrix deposition and osteocytogenesis were initially characterized. Subsequently, the relative influence of biochemical ( $\beta$ -glycerophosphate ( $\beta$ GP) and ascorbic acid 2-phosphate (AA2P)) and mechanical stimulation on osteocytogenesis was compared, with intermittent application of low magnitude FSS generated by see-saw rocker.

**Results:**  $\beta$ GP and AA2P supplementation were required for mineralization and osteocytogenesis, with 33°C cultures retaining a more osteoblastic phenotype and 37°C cultures undergoing significantly higher osteocytogenesis.  $\beta$ GP concentration positively correlated with calcium deposition, whilst AA2P stimulated alkaline phosphatase (ALP) activity and collagen deposition. We demonstrate that increasing  $\beta$ GP concentration also significantly enhances osteocytogenesis as quantified by the expression of green fluorescent protein linked to Dmp1. Intermittent FSS (~0.06 Pa) rocker had no effect on osteocytogenesis and matrix deposition.

**Conclusions:** This work demonstrates the suitability and ease with which IDG-SW3 can be utilized in osteocytogenesis studies. IDG-SW3 mineralization was only mediated through biochemical stimuli with no detectable effect of low magnitude FSS. Osteocytogenesis of IDG-SW3 primarily occurred in mineralized areas, further demonstrating the role mineralization of the bone extracellular matrix has in osteocyte differentiation.

## ARTICLE HISTORY

Received 29 January 2024

Revised 25 June 2024

Accepted 26 June 2024

## KEYWORDS



Matrix mineralization; mechanobiology; biomechanics; bone tissue engineering; extracellular matrix

## 1. Introduction

Bone strength is maintained through the continuous process of osteoblasts forming new bone tissue and osteoclasts breaking down existing bone matrix.<sup>1,2</sup> This process is referred to as bone remodeling. Osteoblast and osteoclast activity are thought to be regulated via paracrine signaling from the highly mechanosensitive osteocytes which are located within the bone tissue.<sup>3</sup> However, for osteoblasts to respond to these signals and deposit bone matrix, several other stimuli are also known to be important.

Biochemistry of the surrounding microenvironment governs bone formation. Ascorbic acid is known to be essential for the assembly of collagen fibers due to its

acting as a co-factor for enzymes associated with collagen fibril assembly,<sup>4,5</sup> whilst phosphate is necessary for hydroxyapatite deposition.<sup>6</sup> The mechanical environment is also known to control bone biology. *In vivo*, bone cells are subjected to a wide range of mechanical forces, such as compression, strain, hydrostatic pressure, and fluid shear stress (FSS). FSS is induced by fluid flow within the porous bone matrix which is driven by small bone deformations due to gravitational and muscle forces<sup>7</sup> and is widely regarded as a potent mechanical stimulus for bone cells.<sup>8-11</sup> A relatively high wall shear stress of approximately 0.8 Pa to 3 Pa is predicted to be generated during physical activity within the microporous lacunar-canalicular system

**CONTACT** Robert Owen  robert.owen@nottingham.ac.uk  Department of Materials Science and Engineering, University of Sheffield, University of Nottingham Biodiscovery Institute, University Park, Nottingham NG7 2RD, UK

\*Claudia Wittkowske is a joint first author

This article has been corrected with minor changes. These changes do not impact the academic content of the article.

© 2024 The Author(s). Published by Informa UK Limited, trading as Taylor & Francis Group.

This is an Open Access article distributed under the terms of the Creative Commons Attribution License (<http://creativecommons.org/licenses/by/4.0/>), which permits unrestricted use, distribution, and reproduction in any medium, provided the original work is properly cited. The terms on which this article has been published allow the posting of the Accepted Manuscript in a repository by the author(s) or with their consent.

where the osteocytes are located;<sup>12</sup> the effect of FSS on this highly mechanosensitive cell type has been the focus of the majority of bone mechanobiology research in the past.<sup>13–16</sup>

Less is known about the effect of FSS on osteoblasts that are in regions with larger porosities, such as the trabeculae. Here, in comparison to osteocytes, the more open and varied geometry of the microenvironment and differences in cell morphology make it more difficult to estimate the type and magnitude of fluid flow osteoblast experience. However, it is assumed that in comparison to osteocytes, the magnitude of the FSS would be much lower and comparable to that of interstitial fluid outside the lacunar-canalicular network.<sup>1</sup>

Studying the immediate and short-term effects of FSS on osteoblasts *in vitro* can be undertaken with relative simplicity as responses typically happen within a short time frame, with the activation of intracellular calcium signaling occurring instantaneously at the onset of flow and signaling molecule release such as prostaglandins occurring within the hour.<sup>17</sup> Assessment of osteocyte calcium signaling *in vivo* in response to mechanical load has also been achieved with multiphoton microscopy.<sup>18</sup> *In vitro*, the magnitude and type of fluid flow have been identified as important regulators for these responses,<sup>19–22</sup> and these signaling cascades are thought to then trigger other bone formation processes such as collagen deposition and mineralization. However, the mechanisms by which these immediate responses translate into the much slower osteogenic processes are less well understood.<sup>23</sup>

The difficulty of understanding the effects of FSS on bone formation *in vitro* is, in part, due to the challenge of maintaining controlled fluid flow over long periods of time (weeks). Microfluidic systems have previously been used,<sup>24</sup> but over extended periods of time the channels become obstructed by proliferating, matrix-depositing osteoblasts, altering the FSS applied. Other flow application methods circumvent these technical challenges, for example the use of parallel-plate flow chambers which can be disassembled following flow application,<sup>25</sup> or systems which consist of relatively large flow channels with a height in the millimeter instead of micrometer range.<sup>26</sup> However, these approaches are demanding to set up and can only apply very low shear stresses, respectively. An alternative to these methods for long-term, dynamic cell culture is to grow cells in multi-well plates on a see-saw rocking platform.<sup>27</sup> Compared to parallel-plate systems, this approach is easy to set up and allows high-throughput testing, although achievable FSS is lower ( $\tau_{\max} \sim 0.06$  Pa) even when using the largest diameter well plates which generate the highest FSS. These

challenges with applying FSS *in vitro* and the range of bone cell types used in studies mean that data on long-term osteogenesis under controlled fluid stimulation are limited and contradictory, with some studies reporting no change in mineralization,<sup>28</sup> while others state a significant increase in collagen and mineral deposition in response to fluid flow.<sup>27,29</sup>

IDG-SW3 is a relatively recently developed cell line that allows the study of osteocytogenesis: the differentiation of osteoblasts to late osteocytes. Alternative cell lines for studying this transition, such as MLO-A5 or MLO-Y4, have limitations such as an absence of key osteocyte proteins or an inability to produce mineralized matrix.<sup>30</sup> IDG-SW3 was developed with the aim of overcoming these limitations due to the importance of matrix mineralization in osteocytogenesis,<sup>31</sup> and as such has the potential to be one of the most effective tools for studying osteocytogenesis *in vitro* currently available. They are derived from transgenic mice where the dentin matrix phosphoprotein-1 (Dmp1) promoter drives the expression of the green fluorescent protein (GFP) in osteocyte-like cells,<sup>30</sup> allowing osteocytes to easily be identified in culture. Dmp-1 is a marker for osteocyte differentiation<sup>32</sup> and is critical for proper mineralization of bone.<sup>33</sup> The role of FSS in osteocytogenesis is of interest as it is hypothesized that enhanced bone formation also accelerates osteocytogenesis as previous research suggests that mineralization may be a trigger for osteoblast to osteocyte differentiation.<sup>34–38</sup>

This study aims to provide a better understanding of how osteoblasts are affected during extended (weeks) time periods by FSS mechanical stimulation using the see-saw rocking method. Culturing IDG-SW3 in this experimental setup allows any effects on both bone formation and osteocytogenesis to be revealed, and in addition to mechanical stimulation, the effects of biochemical and temperature stimulation on bone formation and osteocytogenesis are also characterized for the first time in this cell line.

## 2. Materials and methods

All materials were purchased from Sigma-Aldrich, UK, unless otherwise stated.

### 2.1. IDG-SW3 culture

The murine osteoblast-late osteocyte IDG-SW3 cell line (Kerafast, USA) was used for all experiments between passages 18 and 36. At 33°C in the presence of interferon- $\gamma$  (IFN- $\gamma$ ), these cells express a temperature-sensitive mutant of a tumor antigen

that induces continuous proliferation and immortalization, but at 37°C without IFN- $\gamma$  they resume typical, non-cancerous, osteoblast/osteocyte behavior.<sup>30</sup>

Basal media (BM) consisted of minimum alpha medium with ultraglutamine and nucleosides (Lonza, UK, cat# BE12-169F) supplemented with 10 vol% fetal bovine serum (Labtech, UK (FBS)), 100 units/ml penicillin, and 100  $\mu$ g/ml streptomycin. Cells were passaged according to supplier instructions in expansion media (EM) consisting of BM supplemented with 50 units/mL IFN- $\gamma$  (Gibco, UK) at 33°C in a humidified incubator with 5% CO<sub>2</sub>.

For experiments, cells were plated below confluence (either 10,000 or 25,000 cells/cm<sup>2</sup>) in 0.1% gelatin-coated plates and maintained at 33°C in EM until confluent (day 0). Then, excluding experiments where effects of temperature were investigated, cells were transferred to a 37°C environment and culture medium was replaced with supplemented media (SM), consisting of BM supplemented with 5 mM  $\beta$ -glycerophosphate ( $\beta$ GP) and 50  $\mu$ g/ml L-ascorbic acid 2-phosphate (AA2P) to permit bone formation and osteocytogenesis. As flow experiments were conducted outside the cell culture incubator (5% CO<sub>2</sub>), culture medium was further supplemented with 25 mM HEPES buffer to maintain constant pH at ambient CO<sub>2</sub> conditions. Culture medium was changed for all experiments every 2 to 3 days.

## 2.2. Characterisation of the role of temperature and media composition

Due to the recent development of IDG-SW3 cells, there are a limited number of publications reporting their use (52 PubMed results June 2024). In comparison to other bone cell lines, they require unconventional culture temperatures and media formulations; therefore, the effects of these parameters were initially investigated. To characterize their effects on IDG-SW3 bone formation and osteocytogenesis, cells were maintained from day 0 at either 33°C in EM or SM or at 37°C in EM or SM for 21 days.

**Table 1.** Experimental conditions for biochemical stimulation of IDG-SW3 with AA2P and  $\beta$ GP.

Condition	AA2P ( $\mu$ g/ml)	$\beta$ GP (mM)
#1 (Standard)	50	5
#2	50	10
#3	50	4
#4	50	2.5
#5	50	0
#6	0	0

## 2.3. Biochemical stimulation

To assess the effects of biochemical stimuli on IDG-SW3, the concentrations of  $\beta$ GP and AA2P were varied in the SM applied on day 0 (Table 1). All conditions were compared to the control group which was cultured in our standard SM (50  $\mu$ g/ml AA2P, 5 mM  $\beta$ GP).<sup>27,39–41</sup>

## 2.4. Mechanical stimulation

Cells were subjected to temporally and spatially varying oscillatory FSS 5 days a week using two different rocking frequencies on a see-saw rocker (Stuart, UK) from day 0. The maximum shear stress  $\tau$  at the center of a 6-well plate when the plate was in a horizontal position was estimated using Equation 1:<sup>42</sup>

$$\tau = \frac{\pi\mu\theta_{max}}{2\delta^2 T} \quad (1)$$

where  $\mu$  is the fluid viscosity (10<sup>-3</sup> Pa s),  $\theta_{max}$  is the maximal tilt angle (7°),  $\delta$  is the ratio of the fluid depth in the well to the well diameter, and  $T$  is the time for one cycle (in seconds). Rocking parameters were selected to achieve a “low” and “high” shear stress condition based on previous rocking studies.<sup>27,43–47</sup> Each well was filled with 2 ml of standard SM supplemented with 25 mM HEPES buffer. This resulted in a fluid depth of 2.08 mm in circular 6-well plates with a diameter of 35 mm;  $\delta$  was calculated to be 0.06. The lower rocking frequency of 0.7 Hz generated a maximum shear stress of 0.038 Pa at the base of the well and was applied for either 1 h or 5 h per day. The higher frequency of 1 Hz was applied for 1 h per day and generated a maximum shear stress of 0.054 Pa. Fluid flow experiments were performed in an egg incubator (Rcom, USA) placed on a rocker to maintain a constant temperature of 37°C. Static controls were cultured in standard SM supplemented with HEPES and placed in a non-rocked egg incubator for 1 h per day.

## 2.5. Mineralised matrix deposition

Calcium and collagen deposition were quantified by alizarin red S (ARS) and direct red 80 (DR80) staining, respectively, as previously described.<sup>48</sup> Samples were fixed with 10% formalin for 20 min then washed three times with deionized water. ARS solution (1% w/v) was added to each sample and incubated for 1 h at room temperature to stain calcium. Excess ARS was removed, and samples washed with deionized water until wash water remained clear. Calcium deposits were imaged

with a digital camera before quantification by destaining with 5% perchloric acid for 15 min on an orbital shaker at 100 rpm. Absorption of each sample was measured in triplicate at 405 nm in a clear 96-well plate in a microplate reader (Tecan, CH). Subsequently, samples were washed four times with deionized water before DR80 staining (1 w/v% in saturated picric acid) for collagen for 1 h. Excess DR80 was removed, and samples washed until wash water remained clear. Stained collagen matrices were imaged before quantification by destaining with 0.2 M sodium hydroxide and methanol in a 1:1 ratio for 15 min on an orbital shaker at 100 rpm. Absorption of the destain solution was measured in triplicate at 540 nm.

### **2.6. Assessment of collagen deposition with second harmonic generation imaging**

For biochemical and flow studies, second harmonic generation (SHG) images of fixed cells at day 21 were obtained using a Zeiss LSM 510 Meta upright confocal microscope (Zeiss, DE) equipped with a tuneable (700 nm to 1060 nm) Chameleon Ti:sapphire multi-photon laser. Images were taken using an excitation wavelength of 800 nm and a 40× water immersion objective. SHG emissions were collected in the backward scattering direction filtered through a 10 nm bandpass filter centered on 400 nm.

### **2.7. Assessment of metabolic activity**

PrestoBlue™ Cell Viability agent (ThermoFisher, UK) was used to quantify cell metabolic activity according to manufacturer's instructions. Briefly, media was replaced with PrestoBlue™ working solution (10% PrestoBlue™ in BM) and incubated at 37°C for 1 h. The solution was then transferred to a black 96-well plate and fluorescence detected at  $\lambda_{ex}$ : 560 nm,  $\lambda_{em}$ : 590 nm in a microplate reader (Tecan Infinite 200, Switzerland), where fluorescence correlates with metabolic activity.

### **2.8. Total DNA and alkaline phosphatase activity quantification**

DNA and alkaline phosphatase (ALP) were released from cell cultures by refrigerating overnight in cell digestion buffer (0.15 M Trizma® hydrochloride pH 8.8, 100  $\mu$ M ZnCl<sub>2</sub>, 100  $\mu$ M MgCl<sub>2</sub>, and 1 vol% Triton X-100). Wells were scraped using a cell scraper and the lysates transferred to a microcentrifuge tube before vortexing and freeze-thawing three times (10 min at -80°C, 15 min at 37°C). Lysates were then centrifuged at 10,000 g for 5 min before homogenizing the supernatant. Total DNA was determined with the Quant-it

PicoGreen dsDNA assay kit (Life Technologies, UK) according to manufacturer's instructions. Briefly, 10  $\mu$ L of lysate was combined with 90  $\mu$ L of substrate in a black 96-well plate. Plates were shaken to aid DNA-substrate conjugation, incubated for 10 min at room temperature, then shaken again before measuring fluorescence using a microplate reader (485 nm excitation, 520 nm emission, Tecan Infinite 200, Switzerland). ALP activity was quantified using the Pierce™ PNPP substrate kit (ThermoFisher Scientific, UK) according to manufacturer's instructions. Briefly, 20  $\mu$ L of lysate was combined with 180  $\mu$ L of substrate in a 96-well plate. The change in absorbance at 405 nm was recorded every 60 s for 30 min using a microplate reader (Tecan Infinite 200, Switzerland). Activity is expressed as nmol of p-nitrophenol per minute (nmol pNP/min), assuming one absorbance value equals 19.75 nmol of product. This activity was normalized to the amount of DNA to allow cellular level comparisons.

### **2.9. Assessment of osteocytogenesis**

The transformation from osteoblast-like cells to osteocyte-like cells was assessed by measuring the expression of the fluorescent Dmp1-GFP marker. To determine GFP fluorescence in live cells, culture medium was exchanged for Hank's Balanced Salt Solution (HBSS) before reading fluorescence in top reading mode at 36 locations per well using a microplate reader (485 nm excitation, 535 nm emission, Tecan Infinite 200, Switzerland) with the well plate lid removed. Control values from cell-free wells containing HBSS were subtracted from each reading. Exceptionally high or low readings caused by cell layer detachment were excluded from further analysis.

### **2.10. Microscopy**

Phase-contrast and fluorescence images were obtained with a Ti-E Nikon inverted microscope (Nikon). GFP signal was detected using a filter system with 470 nm excitation, 525 nm emission, and a 2 s exposure time. Cell nuclei were imaged (350 nm excitation, 460 nm emission, 100 ms exposure) after fixed samples were stained for 30 min with 4',6'-diamidino-2-phenylindole (DAPI) solution (BD Biosciences) at a concentration of 5  $\mu$ g/ml. Image analysis was performed with ImageJ.<sup>49</sup>

### **2.11. Statistical analysis**

Data are expressed as mean  $\pm$  standard deviation (SD). Number of replicates for each experiment are provided in the figure legends. Graphical representation and statistical analysis were performed using GraphPad

Prism. One- or two-way analysis of variance (ANOVA) was performed depending on the number of independent variables, with Bonferroni's multiple comparisons test used to identify significant differences.  $p < 0.05$  (\*) was considered significant, and  $p$  values  $< 0.01$  are noted as \*\*.

### 3. Results

#### 3.1. Culturing at 33 °C holds IDG-SW3 in their osteoblastic phenotype

As expected, due to the thermal control of the tumor antigen, the greatest amount of DNA was observed in cultures maintained at 33°C in expansion media (33C EM), with 33C EM having 2.5× more DNA than cultures maintained at 37°C in expansion media (37C EM) on day 7 (Figure 1(a)). On days 14 and 21, there was no significant difference in DNA content at 37°C, regardless of media composition.

The highest normalized ALP activity occurred in cells cultured in supplemented media (SMs), with no significant additional effect of temperature in this media type on days 7 and 14. However by day 21, whereas cells maintained at 37°C in supplemented media (37C SM) underwent a decrease in ALP activity in comparison to day 14 (as associated with osteocytogenesis), cells maintained at 33°C in supplemented media (33C SM) saw an increase in normalized ALP activity in comparison to day 14 and had significantly higher ALP activity than cells maintained 37C SM, indicating they were being held in an osteoblastic phenotype (Figure 1(b)).

This observation agrees with direct osteocytogenesis quantification measured by GFP expression, which had no significant differences until days 21 and 28 when supplemented media cultures were significantly higher than expansion media cultures, and 37C SM was significantly higher than 33C SM at both time points – 4.25× greater on day 28 ( $p < 0.01$ ) (Figure 1(c)).

Furthermore, this retention of osteoblast behavior was observed when determining calcium deposition, which was significantly higher than all other groups on both day 21 and day 28 in 33C SM, with 37°C SM only being significantly higher than EM cultures on day 28 (Figure 1(d,e)).

#### 3.2. Omission of ascorbic acid reduced collagen deposition and ALP activity

None of the biochemical treatment parameters detailed in Table 1 had a significant effect on cell proliferation

as determined by metabolic activity between day 0 and 21 (Figure 2(a)) and the total amount of DNA per well at day 21 (Figure 2(b)). Therefore, significant reduction in normalized ALP activity when AA2P was omitted from the media is a result of lower ALP expression rather than a change in cell number (Figure 2(c)). As expected, the amount of collagen deposited was very low unless ascorbic acid 2-phosphate was present ( $p < 0.05$ ). Visual inspection of the DR80-stained samples confirmed that a layer of collagen was present within the wells, but varying  $\beta$ GP concentration had no effect on the amount deposited (Figure 2(d)).

#### 3.3. Phosphate dose-dependently enhanced mineralisation

IDG-SW3 deposited significant amounts of mineral by day 21 as indicated by a strong ARS staining, with the amount of deposited mineral dependent on  $\beta$ GP concentration (Figure 2(e)). For example, doubling  $\beta$ GP concentration from 5 mM to 10 mM resulted in a 50% increase in mineral deposition ( $p < 0.01$ ). In contrast, reducing  $\beta$ GP concentration resulted in significantly less mineralization ( $p < 0.01$ ). Media without  $\beta$ GP did not support mineralization.

#### 3.4. Osteocyte differentiation in IDG-SW3 is dependent on phosphate concentration and mineralisation

Expression of the osteocyte marker Dmp1, which is linked to GFP fluorescence in IDG-SW3, increased in all culture conditions from day 0 to day 21 ( $p < 0.05$ , data not shown).  $\beta$ GP concentration positively correlated with Dmp1 expression, with higher concentrations of  $\beta$ GP resulting in greater expression of GFP; 10 mM versus 5 mM  $\beta$ GP increased GFP fluorescence by 50% on day 21 (Figure 3(a),  $p < 0.01$ ). In contrast, there was less GFP fluorescence from cells cultured with little or no  $\beta$ GP ( $p < 0.01$ ), with the least GFP fluorescence detected when both  $\beta$ GP and AA2P were omitted ( $p < 0.01$ ). The surface area covered with mineral was higher at greater  $\beta$ GP concentrations. Dmp1-GFP positive cells were primarily located in the mineralized areas, which also had a higher cell density than surrounding areas (Figure 3(b)).

#### 3.5. There was no detectable effect of low fluid shear stress on proliferation or ECM deposition

No significant difference in proliferation was detected between static and mechanically stimulated samples at

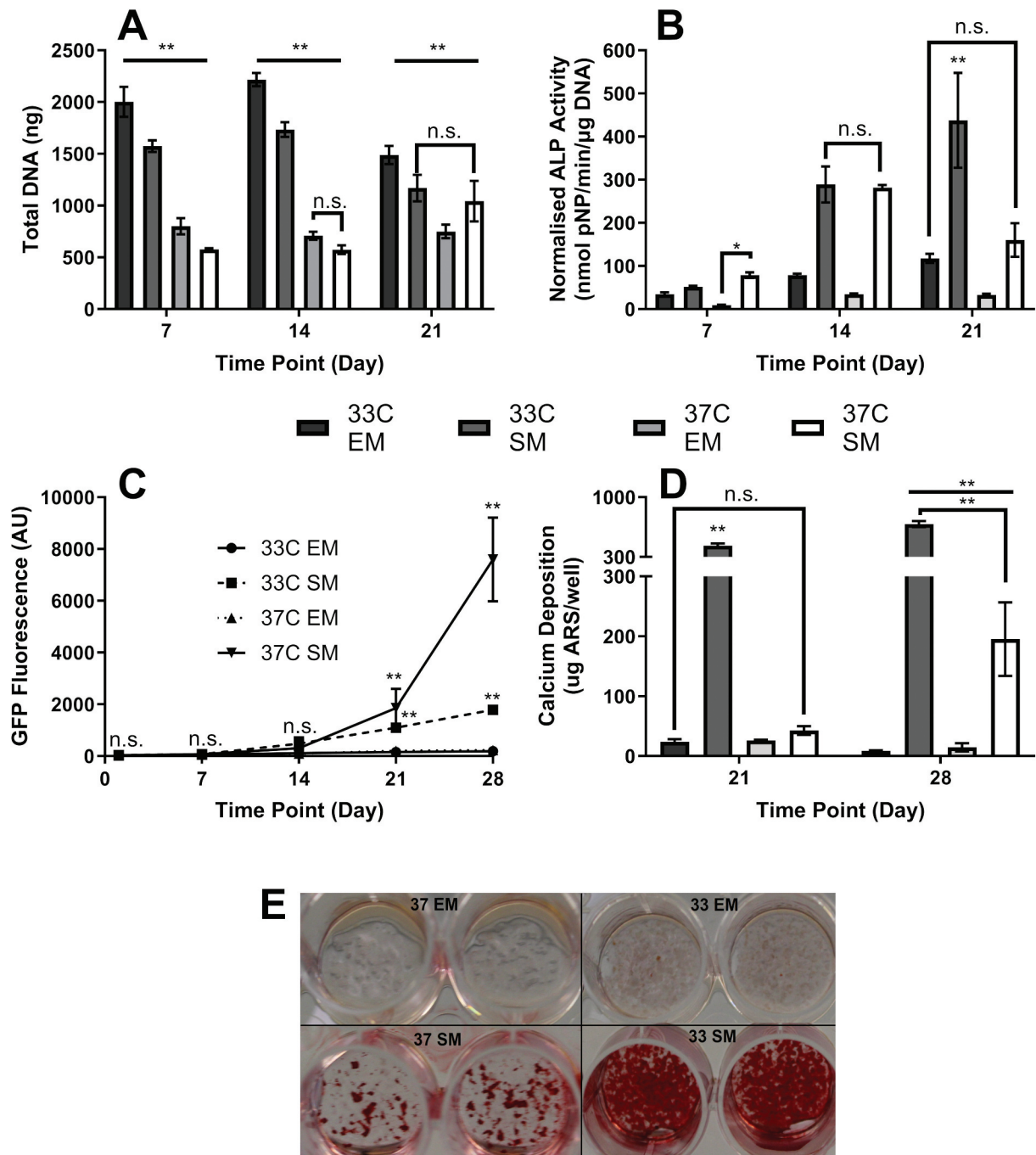


**Figure 1. Effect of culture temperature and media composition.** (a) Total DNA—all groups significantly different at all time points ( $p < 0.01$ ) except day 14 37°C EM vs. 37°C SM and day 21 33°C SM vs. 37°C SM. (b) Normalised ALP activity—no significant difference between the 2 SM cultures on day 14. 33°C SM significantly higher than all other groups on day 21 ( $p < 0.01$ ). No difference between 33°C EM and 37°C SM on day 21. (c) Osteocytogenesis by GFP expression—No significant differences until day 21 when both SM cultures become greater than EM cultures onwards. 37°C SM highest at days 21 and 28. (d) Calcium deposition—significantly higher in 33°C SM at both time points than all other groups. 37°C SM calcium deposition only significantly greater than EM groups on day 28 (all  $n = 4$ ). (e) Representative photograph of ARS staining on day 28. Well diameter 11 mm.

any time point as indicated by metabolic activity (Figure 4(a)) and total DNA (Figure 4(b)), except for the metabolic activity of 0.7 Hz/5 h rocked samples vs. static at day 28. Total DNA significantly increased from the beginning of culture up to day 21 ( $p < 0.01$ ), with

cell numbers plateauing between day 21 and day 28 (Figure 4).

In all conditions, collagen was deposited throughout the whole well and the amount of collagen increased significantly between day 14 and day 28



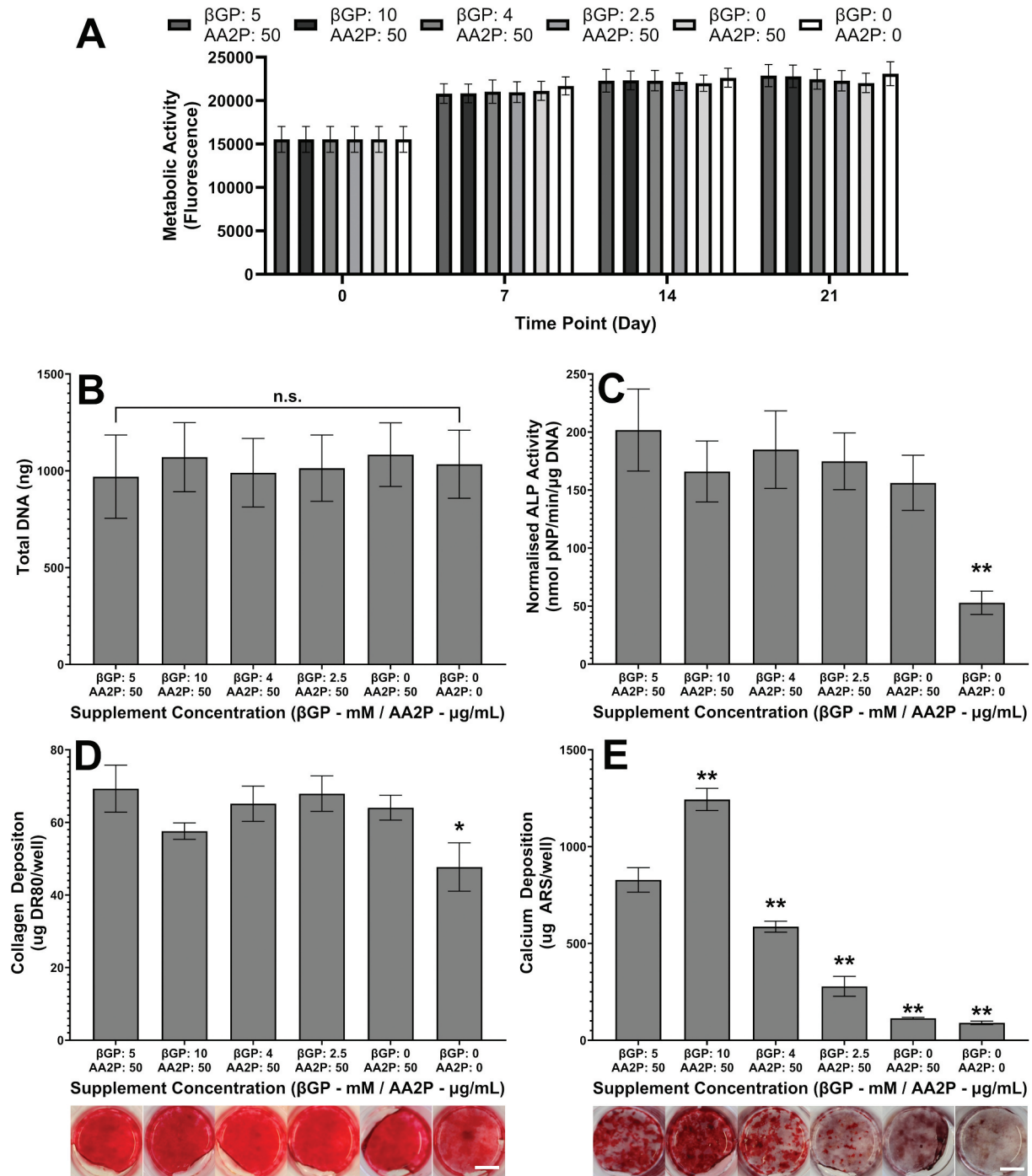


**Figure 2. Effect of biochemical treatment on mineralized matrix formation at day 21.** None of the biochemical treatments had a significant effect on (a) metabolic activity or (b) total DNA over a 21-day period. (c) Normalised ALP activity—omission of AA2P significantly reduced normalized ALP activity through a reduction in ALP expression. (d) Collagen deposition visualized and quantified by DR80. Omission of AA2P resulted in significantly lower deposition of collagen. (e) Calcium deposition visualized and quantified by ARS.  $\beta$ GP dose-dependently enhanced mineralization. Significant differences are compared to standard condition (first column, 5 mM  $\beta$ GP, 50  $\mu$ g/ml AA2P). \* $p < 0.05$ , \*\* $p < 0.01$ ,  $n = 9$ . Scale bar = 7.5 mm.

(Figure 5,  $p < 0.01$ ). Mechanical stimulation at the levels applied did not result in greater collagen deposition at any of the observed time points. Fluorescence microscopy images of DR80 stained samples showed an increase in fiber density over time, thereby

confirming quantitative results from DR80 destaining. The thickness of the collagen layer varied greatly between different locations in the same well and reached up to 20  $\mu$ m as confirmed by SHG imaging. Cell and fiber orientation were not affected by any of

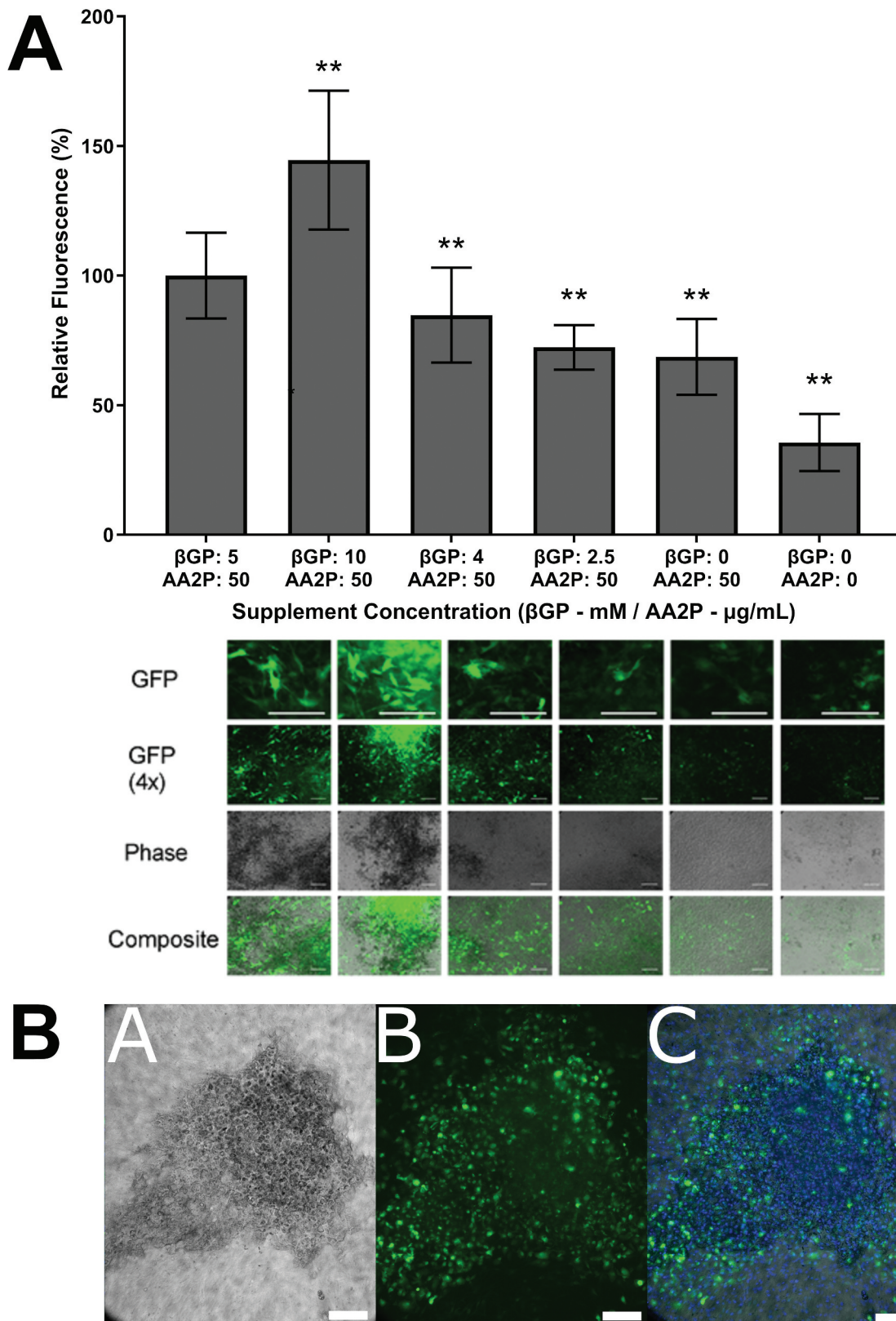


**Figure 3. Effect of biochemical treatment on osteocytogenesis at day 21.** (A—top) Dmp1-GFP expression compared to standard conditions (first column, 5 mM βGP, 50 μg/ml AA2P,  $**p < 0.01$ ,  $n = 9$ ). (A—bottom) Corresponding fluorescence microscope images (scale bars 250 μm). Dmp1-GFP positive cells (green), phase-contrast images show cell contours and mineralized areas in black. (b) Higher magnification image of a mineral nodule showing co-localization of (a) mineralized areas and (b) high concentrations of Dmp1-GFP positive cells. Composite (c) of phase contrast, GFP and nuclei (blue). Scale bars = 200 μm.

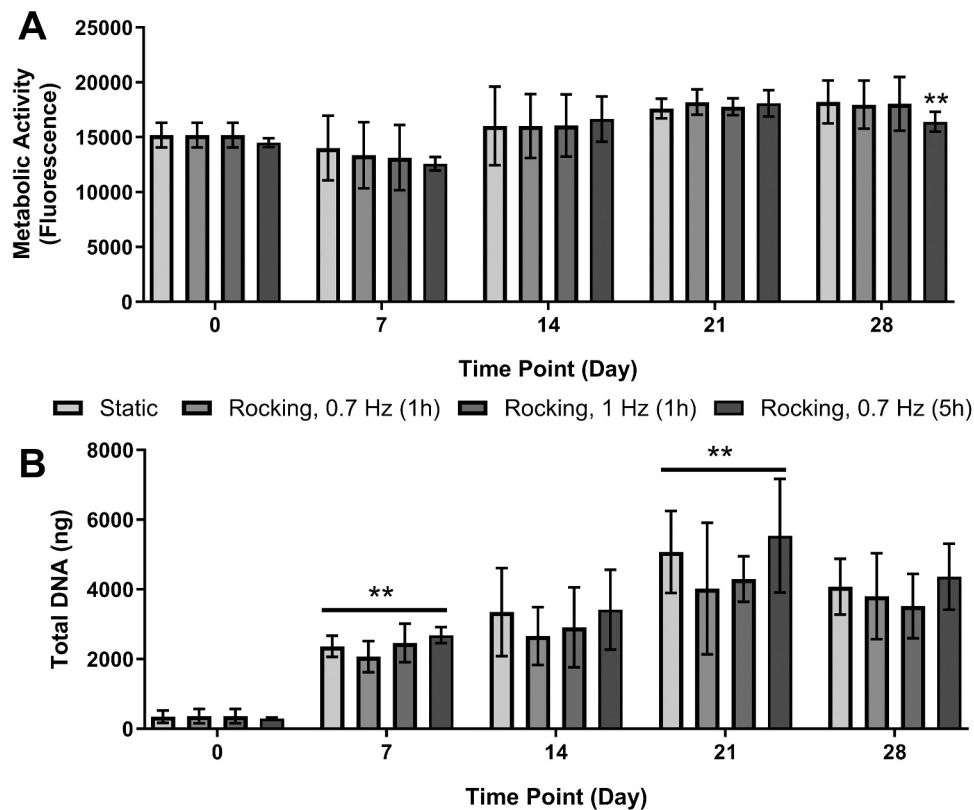


**Figure 4. Effect of low fluid shear stress on proliferation.** No significant difference in (a) metabolic activity between rocked and static samples at any time point except static vs 0.7 Hz/5 h at day 28. (b) Total DNA per sample increased from day 0 to day 21 then plateaued to day 28. No significant differences between static and rocked groups. Significant differences are compared to previous time point. \*\* $p < 0.01$ ,  $n = 9$ .

the tested FSS regimes. Collagen fibers were arranged in honeycomb structures which appeared to be independent of the underlying cell orientation or the direction of fluid flow (Figure 5).

Normalized ALP activity increased in all conditions from day 0 to day 28 (Figure 6(a),  $p < 0.01$ ). However, there was no significant difference in ALP activity between static and mechanically stimulated samples. Mineral deposition significantly increased between day 7 and day 21 in all conditions (Figure 6(b),  $p < 0.01$ ), then plateaued between day 21 and day 28. The amount of mineral was negligible at day 7, with no detectable, red-stained mineral in any of the wells. Rocking did not significantly enhance mineralization compared to the static control group. ARS staining showed that mineral was distributed evenly in the wells.

### 3.6. There was no detectable effect of low fluid shear stress on osteocyte differentiation

Dmp1-GFP fluorescence significantly increased between day 0 and day 28 in all conditions (Figure 6(c),  $p < 0.01$ ), but there was no significant difference between static and mechanically stimulated groups.

Fluorescent images showed that Dmp1-GFP positive cells were primarily located in strongly mineralized areas. Nuclei staining (blue) further indicated that these areas also exhibited the highest concentration of cells. Dmp1-GFP positive cells had spindle-like morphology and often exhibited thin processes (Figure 7).

## 4. Discussion

The aim of this study was to investigate whether FSS enhances bone formation and osteocytogenesis in comparison to biochemical treatments using the osteoblast-osteocyte cell line IDG-SW3. However, unlike more common osteoblast-lineage cell lines such as MC3T3-E1, MLO-A5, and MLO-Y4, IDG-SW3 is cultured in atypical conditions to allow thermal and chemical control over a switch between their proliferating and differentiating state. As there are only a limited number of published studies on IDG-SW3 due to its relatively recent development, before exploring the influence of FSS, a characterization of how IDG-SW3 responds to these different temperature and chemical stimuli was performed.

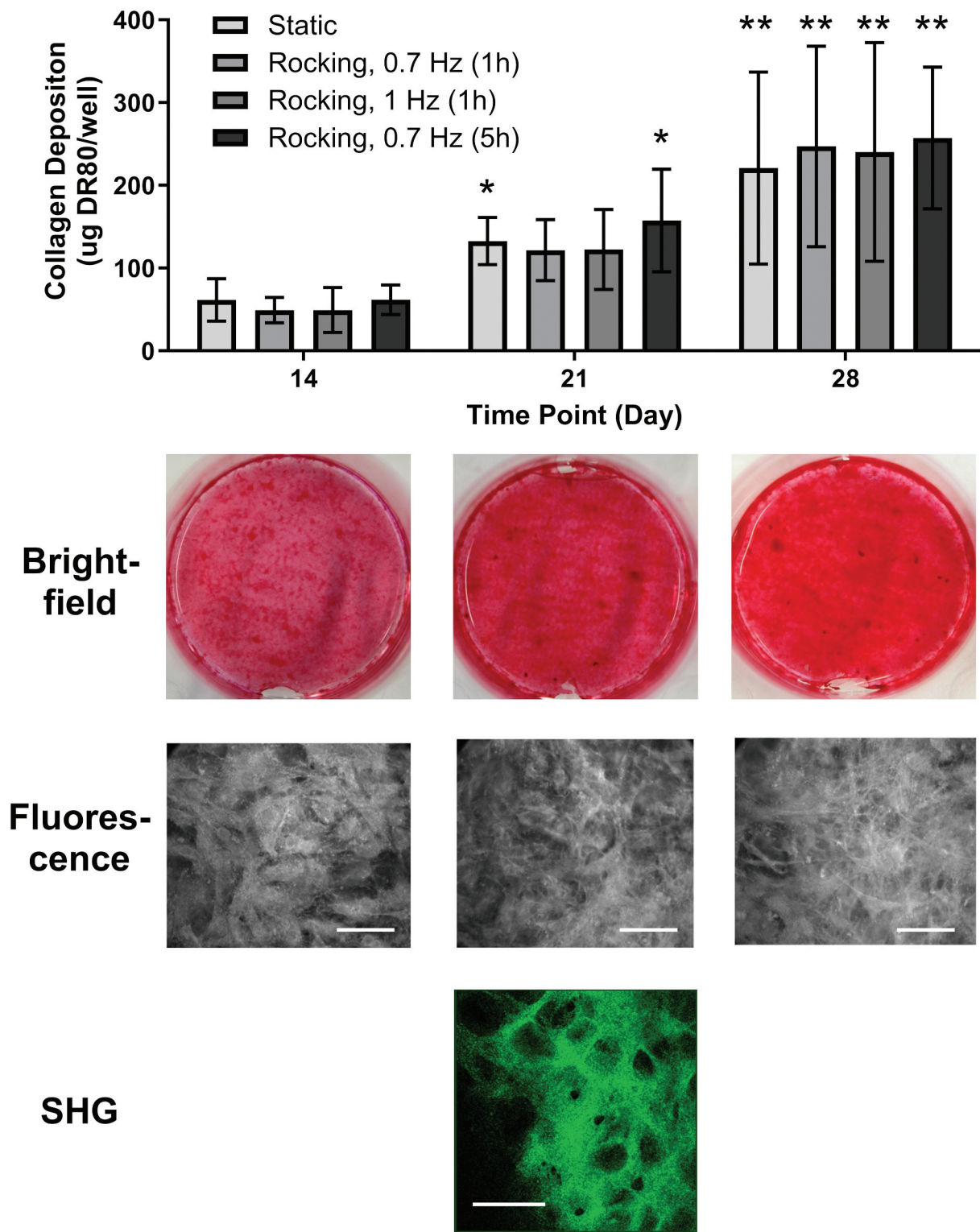


**Figure 5. Effect of low fluid shear stress on collagen deposition.** Top: Quantitative assessment of collagen deposition by DR80 destaining—no significant differences between static and rocked groups. The amount of collagen increased in all conditions from day 14 to day 28 (significant differences are compared to previous time point; \* $p < 0.05$ , \*\* $p < 0.01$ ,  $n = 9$ ). Bottom: Corresponding photographs of static samples. Brightfield images show red stained collagen fibers. Intracellular pro-collagen and extracellular collagen fibers can be visualized with red fluorescent light after staining with DR80. The amount of extracellular collagen fibers increased over time. Extracellular fibers of non-stained samples were visualized with second harmonic generation (SHG) imaging. Extracellular collagen networks formed honeycomb structures which were several micrometers thick. There were no differences in fiber or cell orientation between static and rocked samples. Scale bars = 50  $\mu\text{m}$ .

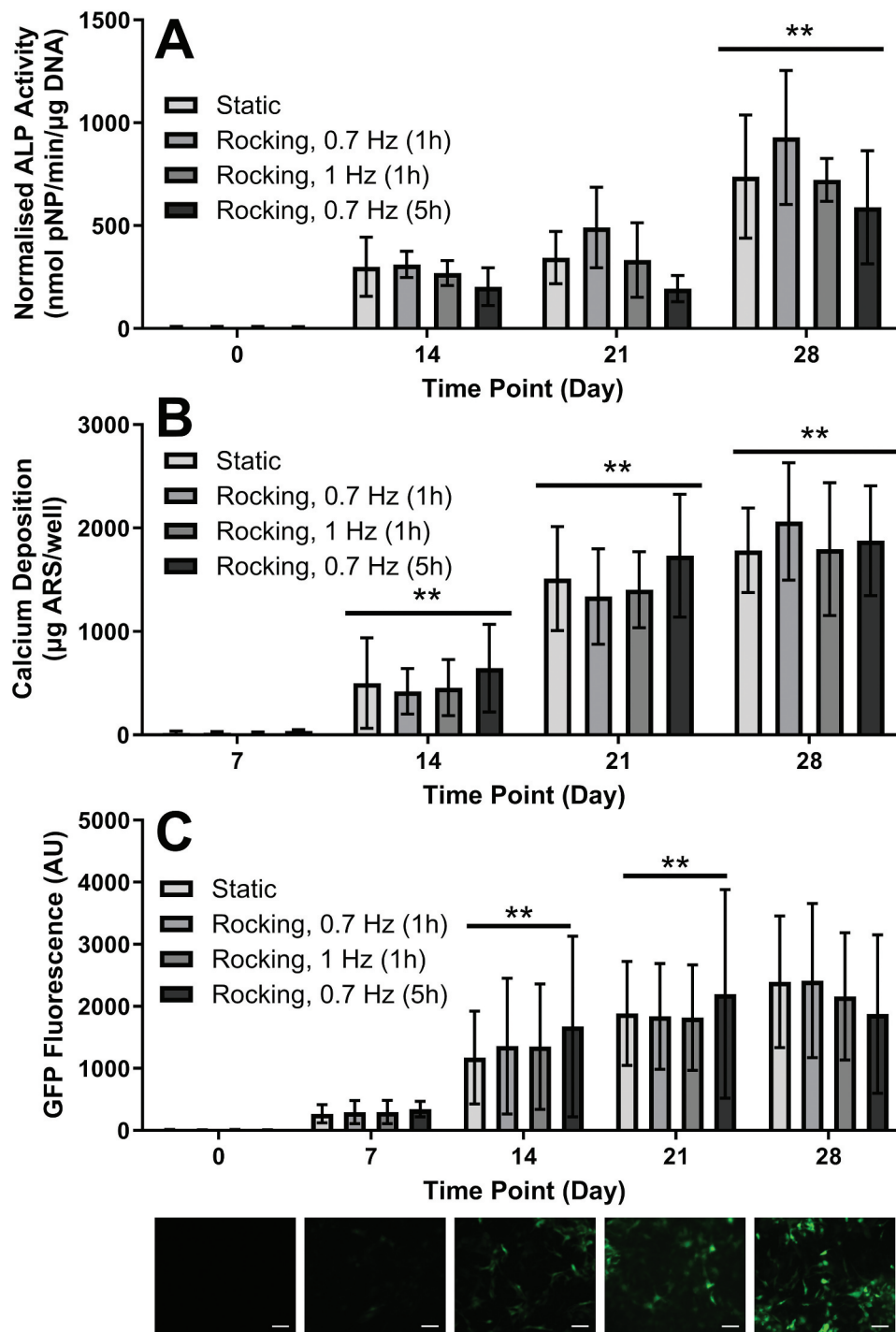


**Figure 6. Effect of low fluid shear stress on ALP activity, mineralization and osteocytogenesis.** (a) Normalised ALP activity increased over time. (b) Calcium deposition increased in all conditions from day 7 to day 28, with the highest increase between day 14 and day 21. For both ALP activity and mineralization, static and rocked conditions were not significantly different. (c—Top) Dmp1-GFP as an osteocyte marker increased significantly over time in all four conditions and was not significantly different between static and rocked samples. (c—Bottom) Corresponding representative fluorescence images from static sample. There were no significant differences in cell orientation, cell morphology and cell distribution between static and rocked samples. Significant differences are compared to previous time point.  $**p < 0.01$ ,  $n = 9$ .

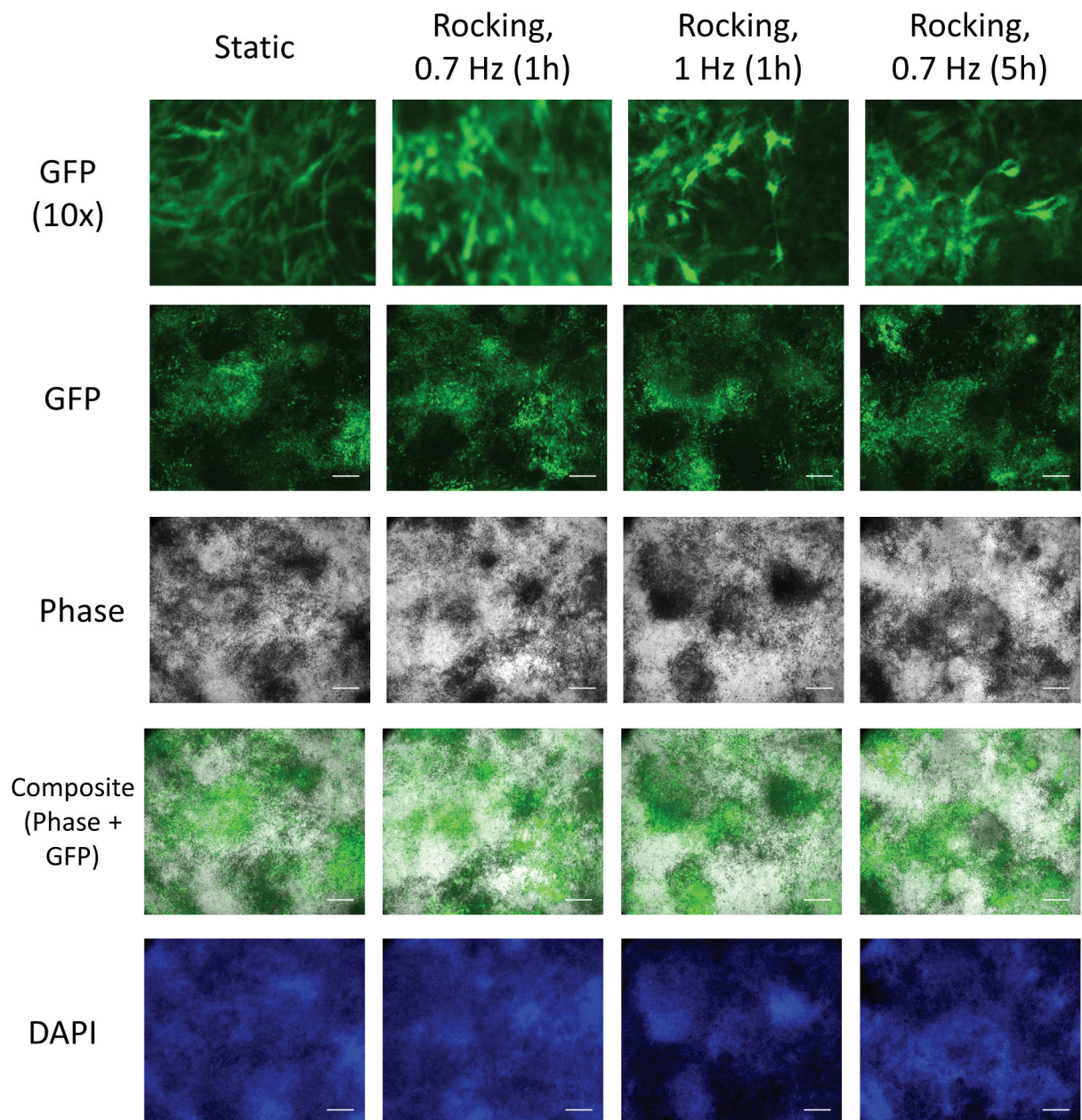


**Figure 7. Co-localization of mineral and Dmp1-GFP positive cells.** In all four conditions mineral deposition and Dmp1-GFP positive cells were co-localized. The black areas in the phase-contrast images are the mineralized areas. Dmp1-GFP positive cells exhibited a spindle-like morphology with processes. A higher concentration of DAPI-stained cell nuclei can be found in mineralized areas. All images were taken at day 28 and are representative ones from the center of a well of three independent experiments. Scale bar = 500  $\mu$ m.

IDG-SW3 is passaged at a lower-than-normal temperature (33°C) in the presence of interferon- $\gamma$  (IFN- $\gamma$ ) to induce expression of a temperature-sensitive mutant of a tumor antigen that induces continuous proliferation and immortalization. When returned to standard culture conditions (37°C, without IFN- $\gamma$ ), this mutant is no longer expressed and IDG-SW3 resumes their normal osteoblast-osteocyte transition. Consequently, it was examined how these two factors (temperature, presence of IFN- $\gamma$ ) affect their osteoblast activity and

osteocytogenesis. As expected, the highest cell numbers were observed when cultures were maintained at 33°C due to the temperature-sensitivity of the SV40 antigen used to control proliferation. Interestingly, even though this mechanism is intended to be controlled by the synergy of the lower temperature and presence of IFN- $\gamma$ , significantly more cells were present at 33°C in IFN- $\gamma$  lacking media than the 37°C cultures, indicating continuous proliferation is still induced at the lower temperature in the absence of IFN- $\gamma$ , albeit at a lower level.

Significantly lower ALP activity was observed in expansion media (EM) cultures regardless of temperature, indicating the importance of  $\beta$ GP and AA2P in the supplemented media (SM) cultures for normal osteoblastic behavior of IDG-SW3. When maintained at 33°C in SM, ALP activity significantly increased at each time point indicating IDG-SW3 cells were being held in an osteoblastic phenotype rather than undergoing osteocytogenesis. In contrast, when maintained at 37°C in SM, ALP activity peaked between day 14 and 21, reducing in the final week as osteocytogenesis proceeded. This is corroborated by Dmp1-GFP fluorescence, with only the SM cultures significantly increasing in fluorescence over time, and the expression in the optimal 37°C supplemented media condition for osteocytogenesis increasing exponentially to levels significantly higher than all other groups.

Unsurprisingly, significant mineralization only occurred in SM groups, but interestingly and again supporting that the osteoblast phenotype is retained at 33°C rather than undergoing osteocytogenesis, much greater calcium deposition occurred at the reduced culture temperature than 37°C. The greater mineralization is likely a result of at least two factors: first, increased proliferation at the lower temperature resulting in earlier confluence and therefore osteoblasts depositing mineralized matrix at an earlier time point in the 33C SM condition, and second, that the greater osteocytogenesis at 37C SM results in a greater number of sclerostin-expressing osteocytes that inhibit mineralization.<sup>30,50</sup> In summary, IDG-SW3 appears to only be able to undergo osteocytogenesis when maintained in conditions that permit mineralized matrix deposition (supplemented media). When maintained in these conditions, mineralized matrix deposition and osteocytogenesis can occur at both 33°C and 37°C, although the greatest matrix deposition occurs at the lower temperature and the greatest osteocytogenesis at the higher temperature. Importantly, despite the requirement for mineralization to occur for osteocytogenesis to be possible, there are diminishing returns; forcing excessive mineralization through 33°C culture does not result in superior osteocytogenesis, instead having an inhibitory effect in comparison to 37°C.

With it established that mineralization is essential for osteocytogenesis to occur, the influence of varying AA2P and  $\beta$ GP concentration on mineralized matrix deposition of IDG-SW3 was investigated. Whilst they had no significant effect on proliferation (Figure 2(a,b)), the deposition of significantly less collagen, lower ALP activity, and negligible mineralization in the absence of AA2P in comparison to AA2P replete media confirmed the vitamin's essential role in osteogenesis (Figure 2(c,e)).

It is required for proper collagen assembly,<sup>4,5</sup> and there is evidence that induction of the osteoblast phenotype and subsequent ALP expression is dependent on the interface between osteoblasts and a collagen-containing extracellular matrix.<sup>51</sup>

With AA2P present, ALP activity was observed to be independent of  $\beta$ GP concentration (Figure 2(c)), although increasing phosphate concentrations significantly increased mineralization (Figure 2(e)), with the greatest calcium deposition observed at 10 mM. The increased mineralization caused by higher concentrations of  $\beta$ GP also enhanced osteocytogenesis (Figure 3(a)), with the greatest number of osteocytes occurring in the most mineralized cultures. Interestingly, the spatial distribution of osteocytes within the cultures overlays almost perfectly onto the regions where mineralized nodules are deposited by the cells (Figures 3(b), 7). This observation indicates that the osteocytogenesis of IDG-SW3 *in vitro* resembles the requirements for osteocytogenesis *in vivo*, where it is currently widely accepted that osteoblasts are self-buried or embedded by neighboring cells into the mineralizing osteoid and as a result experience an environmental stimulation that commits them to becoming osteocytes rather than the other termini of the osteoblast lineage (bone lining cell or apoptosis).<sup>31</sup> Although a  $\beta$ GP concentration of 10 mM gave the greatest osteocytogenesis here and this concentration is often utilized in osteogenic media formulations,<sup>52–54</sup> it has been shown that such high concentrations can result in abnormal, non-osteoblast mediated mineralization caused by spontaneous precipitation of calcium phosphates.<sup>55</sup> Therefore, for subsequent studies investigating the influence of FSS, concentrations of 5 mM were used.

Application of low magnitude FSS using a see-saw rocker had no stimulatory or inhibitory effect on proliferation in comparison to static cultures (Figure 4), which is in line with previous work.<sup>27</sup> Regardless of culture regimen, cell number (total DNA) increased during the first 3 weeks of culture. Since day 0 was defined as the time point when cells reached confluence and therefore IDG-SW3 was transferred to 37°C and SM and FSS were applied, increasing cell number meant that cells tended to form high-density clusters. Continuous proliferation should cease when cultured at 37°C in the absence of INF- $\gamma$ ,<sup>30</sup> however, as observed in Figure 1, some residual proliferation does still occur during the experimental period. This may be the result of a non-immediate deactivation of the tumor antigen that controls proliferation, and as such it can be difficult to tightly control the starting cell number between experimental repeats or laboratory users due to the arbitrary nature of visual estimation of confluence in cell culture.

There was no detectable effect of the applied flow regime on osteogenesis, with no significant changes in collagen production, ALP activity, or calcium deposition of IDG-SW3 (Figure 5, 6). For collagen synthesis, this was not unexpected as there is conflicting information on whether collagen deposition is stimulated under flow, with studies investigating mesenchymal stromal cells<sup>24,56</sup> or the post-osteoblast cell line MLO-A5.<sup>27</sup> indicating minor positive effects, whilst other research has not been able to demonstrate an anabolic effect of flow on collagen at either the mRNA<sup>14</sup> or deposited protein level.<sup>44,47</sup> The application of FSS using see-saw rocking not affecting ALP activity is also consistent with the work of Puwanun et al., which found no effect on the ALP activity of human embryonic derived mesenchymal progenitors, hES-MPs.<sup>44</sup> Whilst mineralized matrix deposition is the parameter most frequently reported to be upregulated by this type of mechanical stimulation on other osteoblast-lineage cell types,<sup>27,44,57</sup> a positive effect is not ubiquitous. In separate work with the same rocker system and comparable shear stresses, MLO-A5 and MC3T3-E1 were shown to also not respond to these levels of FSS, and hES-MPs to a lesser extent than studies using different rocking platforms unless mechanosensitivity is increased through lengthening of the primary cilium via application of lithium chloride.<sup>47</sup>

Considering the close relationship observed thus far between IDG-SW3 mineralization and osteocyte differentiation, it follows that with no enhanced calcium deposition in response to FSS, no effect on osteocytogenesis was observed either. Despite this, in all conditions IDG-SW3 differentiated toward osteocyte-like cells over time as confirmed by increased expression of the osteocyte-marker *Dmp1*.<sup>30,58</sup> We have shown that this temporal change in IDG-SW3 osteocytogenesis is affected by the biochemical environment, although it was not possible to distinguish whether it is the increased mineralization resulting from raised  $\beta$ GP concentration that triggered osteocyte differentiation,<sup>36</sup> or if the greater phosphate concentrations directly stimulated osteocytogenesis.<sup>59</sup> Recent work has shown that inorganic phosphate (Pi) up to concentrations of 1.5 mM released from octacalcium phosphate materials directly stimulated osteocytogenesis in IDG-SW3, but concentrations above this were inhibitory.<sup>60,61</sup>

The lack of detectable response of IDG-SW3 cells to the mechanical stimulation applied here was unexpected due to the widely acknowledged role of osteoblast-lineage cells and especially osteocytes as mechanoresponsive cells. From this study, it seems apparent that osteocytogenesis of IDG-SW3 is coupled to mineralization, and the main driver of this process

is the physical entrapment of the cells within osteoid. The spatial coupling of mineralization to osteocyte formation means it is unlikely that a flow profile could be identified that directly stimulates this terminal differentiation *in absentia* of mineralized osteoid regardless of the magnitude of FSS. However, it is feasible that a different magnitude or methodology of applying FSS to IDG-SW3 could further stimulate mineralized matrix deposition in line with how high concentrations of  $\beta$ GP achieved greater mineralized matrix deposition.

The low magnitude FSS applied in this study may have been below the threshold required to stimulate IDG-SW3; however, the applied magnitude was intentionally low to try and represent the *in vivo* trabecular osteoblast environment.<sup>1</sup> Other studies investigating the response of IDG-SW3 to mechanical stimuli are thus far limited. They have previously been shown to undergo morphological changes in response to high (1.2 Pa) unidirectional FSS, but not low (0.3 Pa) FSS applied in the same manner, but measures of osteocytogenesis were not reported.<sup>62</sup> In that morphology study, the low FSS applied where no response was observed was an order of magnitude greater than that exerted here by the see-saw rocker, which may support that the stimuli were too low here. To date, there are no other studies that looked to mechanically stimulate IDG-SW3 directly with FSS, although when compressed within a 3D hydrogel, the resulting fluid flow within the gel was hypothesized to be the cause of upregulated prostaglandin expression (an approximation of the FSS was not made).<sup>63</sup> Finally, mechanically stretching IDG-SW3 has been shown to downregulate sclerostin, which has the potential to promote mineralization and therefore further osteocytogenesis.<sup>64</sup>

In summary, biochemical treatment with  $\beta$ GP and AA2P, not the application of low magnitude FSS, regulated bone formation and subsequent osteocytogenesis of IDG-SW3. Specifically, the presence of AA2P increased collagen deposition and ALP activity whilst  $\beta$ GP concentration regulated mineralization and mediated osteocytogenesis. This study reveals that the biochemical pathways involved in bone-mineralization may be more influential in the osteoblast-osteocyte transition than low magnitude FSS, and that the presence of mineralizing osteoblasts is essential when studying this process *in vitro*.

## Acknowledgments

The authors wish to acknowledge Dr Nicola Green for helping with the acquisition of SHG images at the Kroto Research Institute Confocal Imaging Facility.



## Disclosure statement

No potential conflict of interest was reported by the author(s).

## Funding

This research was primarily supported by MultiSim, an Engineering and Physical Sciences Research Council (EPSRC) Frontier Engineering Award [EP/K03877X/1], with additional support from the EPSRC (EP/L505055/1, EP/N509735/1), Biotechnology and Biological Sciences Research Council [BB/F016840/1], and Medical Research Council (United Kingdom Regenerative Medicine Platform Hub Acellular Smart Materials 3D Architecture [MR/R015651/1]). RO would like to thank the University of Nottingham for his Nottingham Research Fellowship.

## ORCID

Robert Owen  <http://orcid.org/0000-0003-1961-0733>  
 Claudia Wittkowske  <http://orcid.org/0009-0004-9702-5913>  
 Damien Lacroix  <http://orcid.org/0000-0002-5482-6006>  
 Cecile M. Perrault  <http://orcid.org/0000-0003-2230-6994>  
 Gwendolen C. Reilly  <http://orcid.org/0000-0003-1456-1071>

## References

- Bonewald LF, Johnson ML. Osteocytes, mechanosensing and Wnt signaling. *Bone*. 2008;42(4):606–615. doi:10.1016/j.bone.2007.12.224.
- Hadjidakis DJ, Androulakis II. Bone remodeling. *Ann NY Acad Sci*. 2006;1092(1):385–396. doi:10.1196/annals.1365.035.
- Owen R, Reilly GC. In vitro models of bone remodeling and associated disorders. *Front Bioeng Biotechnol*. 2018;6:134. doi:10.3389/fbioe.2018.00134.
- Canty EG, Kadler KE. Procollagen trafficking, processing and fibrillogenesis. *J Cell Sci*. 2005;118(Pt 7):1341–1353. doi:10.1242/jcs.01731.
- Franceschi RT. The developmental control of osteoblast-specific gene expression: role of specific transcription factors and the extracellular matrix environment. *Crit Rev Oral Biol Med*. 1999;10(1):40–57. doi:10.1177/10454411990100010201.
- Tenenbaum HC, McCulloch CA, Fair C, Birek C. The regulatory effect of phosphates on bone metabolism in vitro. *Cell Tissue Res*. 1989;257(3):555–563. doi:10.1007/BF00221466.
- Owan I, Burr DB, Turner CH, Qiu J, Tu Y, Onyia JE, Duncan RL. Mechanotransduction in bone: osteoblasts are more responsive to fluid forces than mechanical strain. *Am J Physiol*. 1997;273(3):C810–5. doi:10.1152/ajpcell.1997.273.3.C810.
- Klein-Nulend J, Burger EH, Semeins CM, Raisz LG, Pilbeam CC. Pulsating fluid flow stimulates prostaglandin release and inducible prostaglandin G/H synthase mRNA expression in primary mouse bone cells. *J Bone Miner Res*. 1997;12(1):45–51. doi:10.1359/jbmr.1997.12.1.45.
- Verbruggen SW, Sittichokechaiwut A, Reilly GC. Osteocytes and primary cilia. *Curr Osteoporos Rep*. 2023;21(6):719–730. doi:10.1007/s11914-023-00819-1.
- Bonewald LF. Osteocytes as dynamic multifunctional cells. *Ann NY Acad Sci*. 2007;1116(1):281–290. doi:10.1196/annals.1402.018.
- Alfieri R, Vassalli M, Viti F. Flow-induced mechanotransduction in skeletal cells. *Biophys Rev*. 2019;11(5):729–743. doi:10.1007/s12551-019-00596-1.
- Weinbaum S, Cowin SC, Zeng Y. A model for the excitation of osteocytes by mechanical loading-induced bone fluid shear stresses. *J Biomech*. 1994;27(3):339–360. doi:10.1016/0021-9290(94)90010-8.
- Knothe Tate ML, Steck R, Forwood MR, Niederer P. In vivo demonstration of load-induced fluid flow in the rat tibia and its potential implications for processes associated with functional adaptation. *J Exp Biol*. 2000;203(Pt 18):2737–2745. doi:10.1242/jeb.203.18.2737.
- Li YJ, Batra NN, You L, Meier SC, Coe IA, Yellowley CE, Jacobs CR. Oscillatory fluid flow affects human marrow stromal cell proliferation and differentiation. *J Orthop Res*. 2004;22(6):1283–1289. doi:10.1016/j.orthres.2004.04.002.
- Rubin J, Rubin C, Jacobs CR. Molecular pathways mediating mechanical signaling in bone. *Gene*. 2006;367:1–16. doi:10.1016/j.gene.2005.10.028.
- Verbruggen SW, Vaughan TJ, McNamara LM. Fluid flow in the osteocyte mechanical environment: a fluid-structure interaction approach. *Biomech Model Mechanobiol*. 2014;13(1):85–97. doi:10.1007/s10237-013-0487-y.
- Batra NN, Li YJ, Yellowley CE, You L, Malone AM, Kim CH, Jacobs CR. Effects of short-term recovery periods on fluid-induced signaling in osteoblastic cells. *J Biomech*. 2005;38(9):1909–1917. doi:10.1016/j.jbiomech.2004.08.009.
- Lewis KJ, Frikha-Benayed D, Louie J, Stephen S, Spray DC, Thi MM, Seref-Perlenge Z, Majeska RJ, Weinbaum S, Schaffler MB. Osteocyte calcium signals encode strain magnitude and loading frequency in vivo. *Proc Natl Acad Sci USA*. 2017;114(44):11775–11780. doi:10.1073/pnas.1707863114.
- Allen FD, Hung CT, Pollack SR, Brighton CT. Serum modulates the intracellular calcium response of primary cultured bone cells to shear flow. *J Biomech*. 2000;33(12):1585–1591. doi:10.1016/S0021-9290(00)00144-5.
- Hung CT, Pollack SR, Reilly TM, Brighton CT. Real-time calcium response of cultured bone cells to fluid flow. *Clin Orthop Relat Res*. 1995; (313):256–269. [https://journals.lww.com/clinorthop/abstract/1995/04000/real\\_time\\_calcium\\_response\\_of\\_cultured\\_bone\\_cells.35.aspx](https://journals.lww.com/clinorthop/abstract/1995/04000/real_time_calcium_response_of_cultured_bone_cells.35.aspx).
- Huo B, Lu XL, Costa KD, Xu Q, Guo XE. An ATP-dependent mechanism mediates intercellular calcium signaling in bone cell network under single cell nanoindentation. *Cell Calcium*. 2010;47(3):234–241. doi:10.1016/j.ceca.2009.12.005.
- Jacobs CR, Yellowley CE, Davis BR, Zhou Z, Cimbala JM, Donahue HJ. Differential effect of steady versus

- oscillating flow on bone cells. *J Biomech.* 1998;31(11):969–976. doi:10.1016/s0021-9290(98)00114-6.
23. Wittkowske C, Reilly GC, Lacroix D, Perrault CM. In vitro bone cell models: impact of fluid shear stress on bone formation. *Front Bioeng Biotechnol.* 2016;4:87. doi:10.3389/fbioe.2016.00087.
  24. Bahmaee H, Owen R, Boyle L, Perrault CM, Garcia-Granada AA, Reilly GC. Design and Evaluation of an Osteogenesis-on-a-Chip Microfluidic Device Incorporating 3D Cell Culture. *Front Bioeng Biotechnol.* 2020;8:557111. doi:10.3389/fbioe.2020.557111.
  25. Kreke MR, Huckle WR, Goldstein AS. Fluid flow stimulates expression of osteopontin and bone sialoprotein by bone marrow stromal cells in a temporally dependent manner. *Bone.* 2005;36(6):1047–1055. doi:10.1016/j.bone.2005.03.008.
  26. Scaglione S, Wendt D, Miggino S, Papadimitropoulos A, Fato M, Quarto R, Martin I. Effects of fluid flow and calcium phosphate coating on human bone marrow stromal cells cultured in a defined 2D model system. *J Biomed Mater Res A.* 2008;86A(2):411–419. doi:10.1002/jbm.a.31607.
  27. Delaine-Smith RM, MacNeil S, Reilly GC. Matrix production and collagen structure are enhanced in two types of osteogenic progenitor cells by a simple fluid shear stress stimulus. *Eur Cell Mater.* 2012;24:162–174. doi:10.22203/eCM.v024a12.
  28. Nauman EA, Satcher RL, Keaveny TM, Halloran BP, Bikle DD. Osteoblasts respond to pulsatile fluid flow with short-term increases in PGE(2) but no change in mineralization. *J Appl Physiol.* 2001;90(5):1849–1854. doi:10.1152/jappl.2001.90.5.1849.
  29. Morris HL, Reed CI, Haycock JW, Reilly GC, Tanner KE, Dalby MJ. Mechanisms of fluid-flow-induced matrix production in bone tissue engineering. *Proc Inst Mech Eng H.* 2010;224(12):1509–1521. doi:10.1243/09544119JEIM751.
  30. Woo SM, Rosser J, Dusevich V, Kalajzic I, Bonewald LF. Cell line IDG-SW3 replicates osteoblast-to-late-osteocyte differentiation in vitro and accelerates bone formation in vivo. *J Bone Miner Res.* 2011;26(11):2634–2646. doi:10.1002/jbmr.465.
  31. Chen X, Wang L, Zhao K, Wang H. Osteocytogenesis: roles of physicochemical factors, collagen cleavage, and exogenous molecules. *Tissue Eng Part B Rev.* 2018;24(3):215–225. doi:10.1089/ten.teb.2017.0378.
  32. Kalajzic I, Braut A, Guo D, Jiang X, Kronenberg MS, Mina M, Harris MA, Harris SE, Rowe DW. Dentin matrix protein 1 expression during osteoblastic differentiation, generation of an osteocyte GFP-transgene. *Bone.* 2004;35(1):74–82. doi:10.1016/j.bone.2004.03.006.
  33. Lu Y, Yuan B, Qin C, Cao Z, Xie Y, Dallas SL, McKee MD, Drezner MK, Bonewald LF, Feng JQ, et al. The biological function of DMP-1 in osteocyte maturation is mediated by its 57-kDa C-terminal fragment. *J Bone Miner Res.* 2011;26(2):331–340. doi:10.1002/jbmr.226.
  34. Prideaux M, Loveridge N, Pitsillides AA, Farquharson C. Extracellular matrix mineralization promotes E11/gp38 glycoprotein expression and drives osteocytic differentiation. *PLoS One.* 2012;7(5):e36786. doi:10.1371/journal.pone.0036786.
  35. Barragan-Adjemian C, Nicolella D, Dusevich V, Dallas MR, Eick JD, Bonewald LF. Mechanism by which MLO-A5 late osteoblasts/early osteocytes mineralize in culture: similarities with mineralization of lamellar bone. *Calcif Tissue Int.* 2006;79(5):340–353. doi:10.1007/s00223-006-0107-2.
  36. Irie K, Ejiri S, Sakakura Y, Shibui T, Yajima T. Matrix mineralization as a trigger for osteocyte maturation. *J Histochem Cytochem.* 2008;56(6):561–567. doi:10.1369/jhc.2008.950527.
  37. Robin M, Almeida C, Azaïs T, Haye B, Illoul C, Lesieur J, Giraud-Guille M-M, Nassif N, Héлары C. Involvement of 3D osteoblast migration and bone apatite during in vitro early osteocytogenesis. *Bone.* 2016;88:146–156. doi:10.1016/j.bone.2016.04.031.
  38. Welldon KJ, Findlay DM, Evdokiou A, Ormsby RT, Atkins GJ. Calcium induces pro-anabolic effects on human primary osteoblasts associated with acquisition of mature osteocyte markers. *Mol Cell Endocrinol.* 2013;376(1–2):85–92. doi:10.1016/j.mce.2013.06.013.
  39. Sherborne C, Owen R, Reilly GC, Claeysens F. Light-based additive manufacturing of PolyHIPEs: controlling the surface porosity for 3D cell culture applications. *Mater Des.* 2018;156:494–503. doi:10.1016/j.matdes.2018.06.061.
  40. Tetteh G, Khan AS, Delaine-Smith RM, Reilly GC, Rehman IU. Electrospun polyurethane/hydroxyapatite bioactive scaffolds for bone tissue engineering: the role of solvent and hydroxyapatite particles. *J Mech Behav Biomed Mater.* 2014;39:95–110. doi:10.1016/j.jmbbm.2014.06.019.
  41. Wally ZJ, Haque AM, Feteira A, Claeysens F, Goodall R, Reilly GC. Selective laser melting processed Ti6Al4V lattices with graded porosities for dental applications. *J Mech Behav Biomed Mater.* 2019;90:20–29. doi:10.1016/j.jmbbm.2018.08.047.
  42. Zhou X, Liu D, You L, Wang L. Quantifying fluid shear stress in a rocking culture dish. *J Biomech.* 2010;43(8):1598–1602. doi:10.1016/j.jbiomech.2009.12.028.
  43. Lim KT, Kim J, Seonwoo H, Chang JU, Choi H, Hexiu J, Cho WJ, Choung P-H, Chung JH. Enhanced osteogenesis of human alveolar bone-derived mesenchymal stem cells for tooth tissue engineering using fluid shear stress in a rocking culture method. *Tissue Eng Part C Methods.* 2013;19(2):128–145. doi:10.1089/ten.tec.2012.0017.
  44. Puwanun S, Delaine-Smith RM, Colley HE, Yates JM, MacNeil S, Reilly GC. A simple rocker-induced mechanical stimulus upregulates mineralization by human osteoprogenitor cells in fibrous scaffolds. *J Tissue Eng Regen Med.* 2018;12(2):370–381. doi:10.1002/term.2462.
  45. Hoey DA, Kelly DJ, Jacobs CR. A role for the primary cilium in paracrine signaling between mechanically stimulated osteocytes and mesenchymal stem cells. *Biochem Biophys Res Co.* 2011;412(1):182–187. doi:10.1016/j.bbrc.2011.07.072.
  46. Tucker RP, Henningsson P, Franklin SL, Chen D, Ventikos Y, Bompfrey RJ, Thompson MS. See-saw rocking: an in vitro model for mechanotransduction

- research. *J R Soc Interface*. 2014;11(97):20140330. doi:10.1098/rsif.2014.0330.
47. Boyle L. Lithium enhances osteogenic responses to fluid shear stress. Sheffield: University of Sheffield; 2019.
  48. Owen R, Bahmaee H, Claeysens F, Reilly GC. Comparison of the anabolic effects of reported osteogenic compounds on human mesenchymal progenitor-derived osteoblasts. *Bioeng (Basel)*. 2020;7(1):12. doi:10.3390/bioengineering7010012.
  49. Schneider CA, Rasband WS, Eliceiri KW. NIH image to ImageJ: 25 years of image analysis. *Nat Methods*. 2012;9(7):671–675. doi:10.1038/nmeth.2089.
  50. Cosman F, Crittenden DB, Adachi JD, Binkley N, Czerwinski E, Ferrari S, Hofbauer LC, Lau E, Lewiecki EM, Miyauchi A, et al. Romosozumab treatment in postmenopausal women with osteoporosis. *N Engl J Med*. 2016;375(16):1532–1543. doi:10.1056/NEJMoa1607948.
  51. Xiao G, Gopalakrishnan R, Jiang D, Reith E, Benson MD, Franceschi RT. Bone morphogenetic proteins, extracellular matrix, and Mitogen-activated protein kinase signaling pathways are required for osteoblast-specific gene expression and differentiation in MC3T3-E1 cells. *J Bone Miner Res*. 2002;17(1):101–110. doi:10.1359/jbmr.2002.17.1.101.
  52. Burgio F, Rimmer N, Pielele U, Buschmann J, Beaufils-Hugot M. Characterization and in ovo vascularization of a 3D-printed hydroxyapatite scaffold with different extracellular matrix coatings under perfusion culture. *Biol Open*. 2018;7(12). doi:10.1242/bio.034488.
  53. Ingavle GC, Gionet-Gonzales M, Vorwald CE, Bohannon LK, Clark K, Galuppo LD, Leach JK. Injectable mineralized microsphere-loaded composite hydrogels for bone repair in a sheep bone defect model. *Biomaterials*. 2019;197:119–128. doi:10.1016/j.biomaterials.2019.01.005.
  54. Yan Y, Cheng B, Chen K, Cui W, Qi J, Li X, Deng L. Enhanced osteogenesis of bone marrow-derived mesenchymal stem cells by a functionalized silk fibroin hydrogel for bone defect repair. *Adv Healthc Mater*. 2019;8(3):e1801043. doi:10.1002/adhm.201801043.
  55. Schäck LM, Noack S, Winkler R, Wißmann G, Behrens P, Wellmann M, Jagodzinski M, Krettek C, Hoffmann A. The phosphate source influences gene expression and quality of mineralization during in vitro osteogenic differentiation of human mesenchymal stem cells. *PLoS One*. 2013;8(6):e65943. doi:10.1371/journal.pone.0065943.
  56. Stavenschi E, Labour MN, Hoey DA. Oscillatory fluid flow induces the osteogenic lineage commitment of mesenchymal stem cells: the effect of shear stress magnitude, frequency, and duration. *J Biomech*. 2017;55:99–106. doi:10.1016/j.jbiomech.2017.02.002.
  57. Sittichokechaiwut A, Edwards JH, Scutt AM, Reilly GC. Short bouts of mechanical loading are as effective as dexamethasone at inducing matrix production by human bone marrow mesenchymal stem cell. *Eur Cell Mater*. 2010;20:45–57. doi:10.22203/ecm.v020a05.
  58. Feng JQ, Ward LM, Liu S, Lu Y, Xie Y, Yuan B, Yu X, Rauch F, Davis SI, Zhang S, et al. Loss of DMP1 causes rickets and osteomalacia and identifies a role for osteocytes in mineral metabolism. *Nat Genet*. 2006;38(11):1310–1315. doi:10.1038/ng1905.
  59. Rendenbach C, Yorgan TA, Heckt T, Otto B, Baldauf C, Jeschke A, Streichert T, David JP, Amling M, Schinke T, et al. Effects of extracellular phosphate on gene expression in murine osteoblasts. *Calcif Tissue Int*. 2014;94(5):474–483. doi:10.1007/s00223-013-9831-6.
  60. Sai Y, Shiwaku Y, Anada T, Tsuchiya K, Takahashi T, Suzuki O. Capacity of octacalcium phosphate to promote osteoblastic differentiation toward osteocytes in vitro. *Acta Biomater*. 2018;69:362–371. doi:10.1016/j.actbio.2018.01.026.
  61. Saito S, Hamai R, Shiwaku Y, Hasegawa T, Sakai S, Tsuchiya K, Sai Y, Iwama R, Amizuka N, Takahashi T, et al. Involvement of distant octacalcium phosphate scaffolds in enhancing early differentiation of osteocytes during bone regeneration. *Acta Biomater*. 2021;129:309–322.
  62. Xu H, Duan J, Ren L, Yang P, Yang R, Li W, Zhao D, Shang P, Jiang JX. Impact of flow shear stress on morphology of osteoblast-like IDG-SW3 cells. *J Bone Miner Metab*. 2018;36(5):529–536. doi:10.1007/s00774-017-0870-3.
  63. Wilmoth RL, Ferguson VL, Bryant SJ. A 3D, dynamically loaded hydrogel model of the osteochondral unit to study osteocyte mechanobiology. *Adv Healthc Mater*. 2020;9(22):e2001226. doi:10.1002/adhm.202001226.
  64. Sasaki F, Hayashi M, Mouri Y, Nakamura S, Adachi T, Nakashima T. Mechanotransduction via the Piezo1-Akt pathway underlies sost suppression in osteocytes. *Biochem Biophys Res Commun*. 2020;521(3):806–813. doi:10.1016/j.bbrc.2019.10.174.